JMEPEG
https://doi.org/10.1007/s11665-024-09584-3

1059-9495/$19.00

ORIGINAL RESEARCH ARTICLE

The Effect of Heat Treatment and Extrusion on Microstructure and Properties of Medical Mg-1Mn-2Zn Alloy

Kezhen Yuan, Shunheng Sang, Shenjin Lv, Tianzhong Wang, Dongfang Gao, Yangyang Zhao, and Yang Qiao

Submitted: 15 October 2023 / Revised: 5 April 2024 / Accepted: 22 April 2024

Magnesium alloy with its excellent biocompatibility and degradability has been widely used in clinical medical research as a highly promising medical metal material, but when the composition of magnesium alloy is different, the performance of magnesium alloys also has the huge difference. At the same time, the poor mechanical properties and corrosion resistance of cast magnesium alloys do not allow them to be used directly as implants. In this paper, Mg-1Mn-2Zn alloys were prepared by self-research, and the prepared magnesium alloy was subjected to heat treatment and extrusion composite strengthening to improve its performance. The improvement of mechanical properties of magnesium alloy was investigated by hardness, residual stress and tensile bending tests. Then, fretting wear test and electrochemical corrosion test were carried out, and the corrosion products were analyzed. The results show that the mechanical properties and corrosion resistance of the alloy are greatly improved, and the alloy has good degradability and biocompatibility. This provides theoretical guidance and practical guidance for the preparation, strengthening and application of high-performance medical magnesium alloys.

Keywords biocompatibility, corrosion, mechanical property, medical magnesium alloys, strengthening process

1. Introduction

In recent years, due to the gradual development of society and the increasing aging of the population, the number of accidents such as fractures has become increasing. Therefore, the demand for medical materials with excellent properties is also increasing year by year. Magnesium alloy has become a research hotspot of medical metal materials in recent years because of its low density, light weight, high specific strength, good biocompatibility, elastic modulus, compressive strength and density similar to human bone properties (Ref 1-4).

Studies have found that magnesium ions in the human body can induce the division and reproduction of bone cells, and it has excellent bone induction (Ref 5-7). At the same time, alloy elements such as zinc, calcium and manganese are highly nutritious, non-toxic and harmless alloy elements (Ref 8-11). Using these elements to prepare medical magnesium alloy materials is the first choice for implants. However, magnesium alloys cannot be used as implants if they do not have sufficient yield strength, wear resistance and corrosion resistance. Appropriate addition of Zn or Mn to Mg alloys helps to improve the mechanical properties and corrosion resistance of Mg alloys. Yin (Ref 12) investigated the effect of Zn on the organization and mechanical properties of Mg-Mn alloys and found that when the Zn content was increased from 0 to 3 wt.%, the grain size was reduced and the mechanical properties were significantly improved. Němec (Ref 13) investigated the microstructure and compressive properties of Mg alloys with different Zn contents structure and compressive properties. The results showed that the increase in Zn content increases the number of precipitates and compressive strength. Polina (Ref 14) found that the addition of manganese to magnesium alloys helps to refine the microstructure of the alloys, reduces the harmful effects of impurities and enhances the mechanical properties of the alloys. Rosalbino (Ref 15) studied the corrosion resistance of Mg-2Zn-0.2Mn in Ringer's physiological solution and found that the alloys were four times more corrosion resistant than the AZ91 magnesium alloy.

Although magnesium-manganese-zinc alloys have low density and good machinability, the castings have relatively low strength and hardness and are susceptible to thermal and chemical corrosion. Erinc (Ref 16) proposed that the corrosion rate of the material to be implanted in the body fluid should be less than 0.5 mm/a at 37 °C, the strength should be above 200 MPa and the elongation should be higher than 10%. During the healing period of 12 months, the magnesium plate should remain in the body without losing its mechanical integrity (Ref 17). After human bone healing, it should be completely degraded within 12-24 months (Ref 18). According to these requirements, the cast magnesium alloy should be appropriately strengthened. Studies have shown that alloying treatment, heat treatment and plastic deformation of magnesium are extremely effective treatment methods to improve the performance of the alloy (Ref 19-23). Therefore, the mechan-

Kezhen Yuan, Shunheng Sang, Shenjin Lv, Tianzhong Wang, and **Yang Qiao**, School of Mechanical Engineering, University of Jinan, Jinan 250022, China; **Dongfang Gao**, Institute of Medical Sciences, The Second Hospital of Shandong University, Jinan 250033, China; **Yangyang Zhao**, Trauma Orthopedics, The Second Hospital of Shandong University, Jinan 250031, China. Contact e-mail: me_qiaoy@ujn.edu.cn.

Published online: 17 May 2024

ical properties and corrosion resistance of Mg-Mn-Zn alloys can be improved by suitable heat treatment and extrusion strengthening treatment. Sadiq (Ref 24) studied the effect of heat treatment on AZ91 magnesium alloy and found that proper heat treatment can effectively improve the hardness and corrosion resistance of the alloy. Sheng (Ref 25) carried out aging treatment of magnesium alloys at different temperatures and showed that heat treatment increases yield and tensile strength, but elongation decreases. Kiani (Ref 26) studied the effect of extrusion on the microstructure, mechanical properties and corrosion resistance of medical magnesium alloys. The results show that the mechanical properties and corrosion resistance of magnesium alloy are significantly improved by extrusion strengthening. Du (Ref 27) found that the extrusion process can effectively enhance the mechanical properties and corrosion resistance of medical magnesium alloys, and improve the dynamic recrystallization ratio and size within the alloy. Zhang (Ref 28) found that hot extrusion helps Mg-6Zn alloy to obtain better mechanical properties, and the tensile elongation and strength of the alloy can reach 18.8% and 279.5 MPa after extrusion.

In this paper, the self-prepared Mg-1Mn-2Zn alloy was subjected to Heat treatment and extrusion strengthening treatment. The effects of composite strengthening on the mechanical properties, wear resistance and corrosion resistance of magnesium alloy were studied by hardness, residual stress test, tensile bending strength analysis, wear resistance test and corrosion resistance test. It provides a new research idea for the preparation and processing strengthening of medical implanted magnesium alloy.

2. Materials and Test Methods

2.1 Test Materials

In this experiment, the self-made medical Mg-1Mn-2Zn alloy was studied. The preparation materials used were 99.95% pure magnesium block, 99.95% pure zinc and 99.95% pure manganese. The mixture was melted according to the ratio of Mn and Zn to 1 and 2%, respectively. The protective gas SF6 was filled during the melting process. After the material was fully melted and mixed, the material was taken out of the melting furnace and cooled to form a cast Mg-1Mn-2Zn alloy. The cast magnesium-manganese-zinc alloy has a cylindrical shape with dimensions of 500 × Φ100 mm.

2.2 Composite Strengthening Treatment

In this paper, the strengthening method is a combination of heat treatment and extrusion strengthening to improve the performance of cast magnesium alloy as a whole. Firstly, the prepared casting material was strengthened by heat treatment. The heat treatment was carried out by artificial aging (T6) treatment. The material was put into the material at the initial temperature of 360 °C, and then the temperature was increased from 360 to 420 °C. The material was placed in the furnace for 10 h, and then the material was kept for 2 h and cooled naturally.

For the magnesium alloy after heat treatment, the oxide skin on its surface was removed by lathe, and it was processed into a cylinder of Φ48 mm × 30 mm by wire cutting machine and lathe. According to the difficulty of the extrusion process, the extrusion temperature of the material is set to 300 °C, and the extrusion ratio is 9:1. The schematic diagram of the extrusion process is shown in Fig. 1. The extrusion die is self-designed. After the extrusion die and the material are heated to 300 °C, the press is used for extrusion. The material is extruded into a bar with a diameter of 16 mm after passing through the extrusion die.

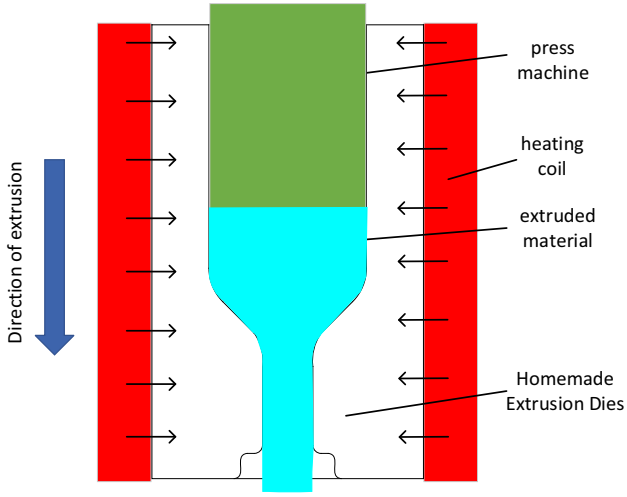

Fig. 1 Extrusion process diagram

2.3 Mechanical Properties Test and Microstructure Analysis of the Alloy

2.3.1 Microhardness Test. The hardness of magnesium manganese zinc alloy castings, heat treatment parts and extrusion parts were tested, respectively. Before the test, the three workpieces were polished step by step with 400#, 800#, 1000#, 1200# and 1500# metallographic sandpaper. After the treatment, the surface was ultrasonically cleaned with alcohol to remove the debris and other impurities on the surface. Then the 402MVD Vickers hardness tester was used to test the hardness. The loading force was set to 50 gf and the loading time was 15 s. The hardness of each workpiece was measured at seven positions, and the maximum and minimum values were removed. Then, the average value of the remaining five microhardness was obtained to ensure the reliability of the results.

2.3.2 Residual Stress Test. The residual stress of the alloy was measured by a residual stress meter. The Cr target was used in the experiment. The parameters were set as follows: Braggle angle 138°, gain voltage 10 kv and exposure time 2. The residual stress of each workpiece was measured at five different positions, and the average value was taken.

2.3.3 Tensile Test and Three-Point Bending Test. The tensile and three-point bending tests were carried out on a microcomputer-controlled electronic universal testing machine (CMT5305). The tensile speed and the loading speed of the indenter were set to 2 mm/min, and the temperature was room temperature. The size of the tensile specimen and the three-point bending specimen of the casting and the heat-treated part was 88 × 24.5 × 3.5 and 70 × 5 × 5, respectively. Due to the limitation of the size of the extruded part after extrusion, the size and shape of the tensile and bending specimens were slightly reduced, which were 84 × 8 × 2.5 and 70 × 4 × 4,

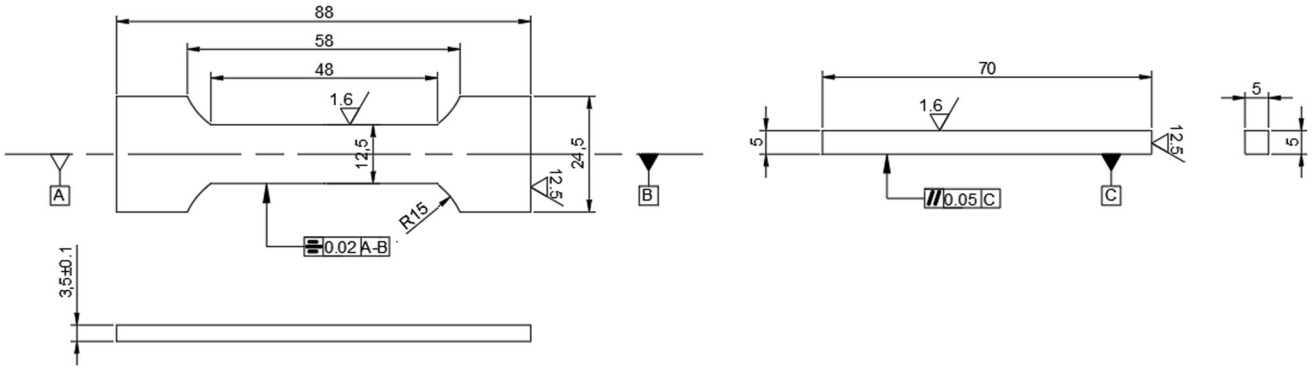

Fig. 2 Specimen shape and size of tensile and three-point bending tests

respectively. In the experiment, the scale distance of the tensile specimen was set to 50 mm, and the span of the three-point bending specimen was 30 mm. The specific shape and size of the sample are shown in Fig. 2. To ensure the reliability of the experiments, four samples of each of the tensile and flexural tests were made for testing.

The tensile test reflects the change of the mechanical properties of the material through the change of the real stress and strain of the material. The real stress and strain of the material is obtained by the engineering stress and strain of the material, and the engineering stress and strain of the material is obtained by the force-displacement curve of the material. The force-displacement curve of the material can be obtained in the experiment. The specific calculation formulas are as (1), (2).

$$\sigma N = \frac{F}{A_0},\ \varepsilon N = \frac{\Delta L}{L_0} \quad \text{(Eq 1)}$$

$$\sigma T = \sigma N(1+\varepsilon N),\ \varepsilon T = Ln(1+\varepsilon N) \quad \text{(Eq 2)}$$

where σN is the engineering stress, F is the force, A_0 is the cross-sectional area of the specimen; εN is the engineering strain, ΔL is the elongation, L_0 is the initial length; σT is the true stress; εT is the true strain.

For the three-point bending test, in order to obtain more accurate results and facilitate the comparative analysis between the results, the strength formula of the three-point bending test is used for calculation to improve the reliability of the results. The formula is shown in (3).

$$R = \frac{3FL}{2bh^2} \quad \text{(Eq 3)}$$

where R is the bending strength, F is the loading force, L is the span, b is the width of the sample, h is the height of the sample.

2.3.4 Fracture Morphology Observation. QUANTA 250 FEG was used to observe the fracture morphology of magnesium alloy after tensile and bending fracture, and the fracture form and performance change of the material were analyzed. Experimental parameters: accelerating voltage 20.0 kV.

2.3.5 XRD Diffraction Analysis. The physical phases present in the Mg-Mn-Zn alloy were analyzed using Cu Kα source x-ray diffraction (XRD, D8ADVANCE, Bruegger, Germany), the XRD equipment was operated under Cu Kα (λ = 0.1541 nm) radiation with a range of 2θ from 10° to 90° with a step size of 5°/min, all the reflections in the figure were identified using the jade software was done.

2.4 Service Performance Test of Alloy

2.4.1 Fretting Wear Test. The fretting wear test of magnesium alloy was carried out by using Rtec MFT-3000 friction and wear tester to simulate the environment of human activities. Before the experiment, according to the actual needs, the surface of magnesium alloy was polished by 800#, 1000#, 1200#, 1500#, 2000# sandpaper to meet the surface roughness requirements. The experimental temperature of fretting wear was set to 37 °C. The grinding ball was GCr15 bearing steel, with a diameter of 9.525 mm, an amplitude of 20 μm, a frequency of 2 Hz, a loading force of 100 N, and a cycle time of 1 h. The friction pair adopts the classical tangential ball/plane contact mode. After the test, the wear debris particles on the surface were removed by ultrasonic cleaning with alcohol for 5 min, and the surface morphology of the wear scar was observed by a white light interferometer.

2.4.2 Corrosion Resistance Test. After the alloy is implanted into the human body, galvanic corrosion will occur in the complex environment of the human body. Therefore, the electrochemical corrosion test is used to evaluate the corrosion degradation behavior of the magnesium alloy after implantation into the human body. Electrochemical tests were performed in simulated body fluid (SBF) using an electrochemical test system (CHI604E). To stabilize the open circuit potential (OCP), each sample was immersed in the electrolyte for 10 min with the scan rate set to 1 mV/s and the potential controlled in the range of (− 2, 0) for the kinetic potential polarization test. A wire cutter was used to make 10 × 10 × 10 mm block of alloy for inlay, only one side of the inlaid magnesium alloy is in contact with the air, and the exposed side of the square was sanded and polished for electrochemical corrosion degradation tests. The electrochemical corrosion degradation test is carried out in a constant temperature water bath at 37 °C.

2.4.3 Analysis of Corrosion Products. The corrosion surface of magnesium alloy was analyzed by XPS using Thermo SCIENTIFIC ESCALAB Xi+ , and the corrosion degradation products of Mg-1Mn-2Zn were analyzed and

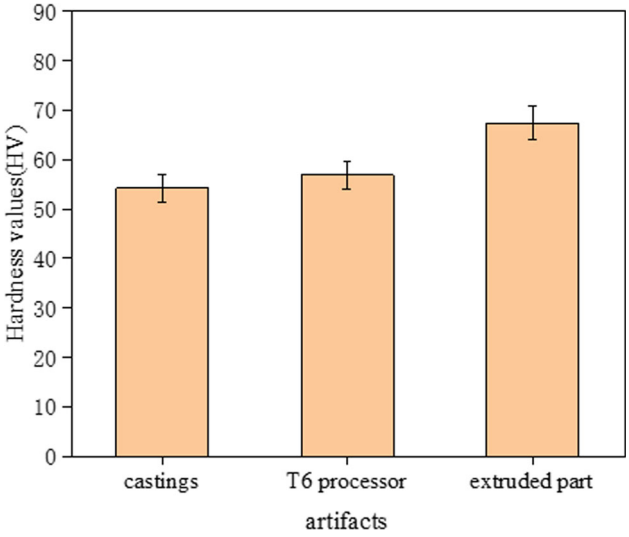

Fig. 3 Comparison of hardness of different treated workpieces

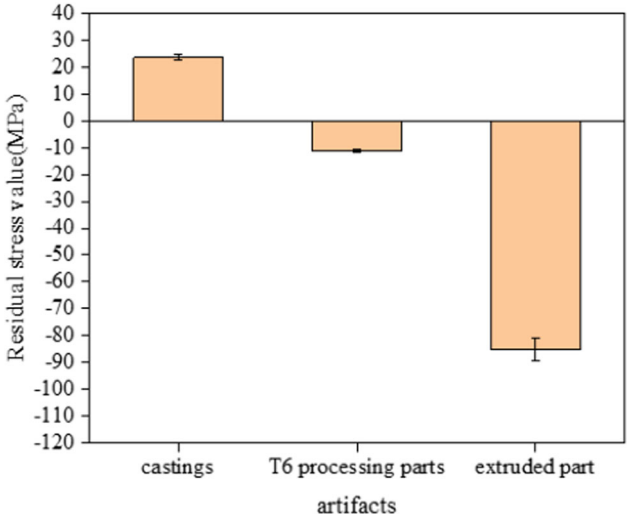

Fig. 4 Comparison of residual stress test of workpieces with different treatments

determined by Advantage software.

3. Results and Analysis

3.1 Hardness Test of Medical Mg-1Mn-2Zn Alloy

Figure 3 shows the comparison of hardness changes of medical Mg-1Mn-2Zn alloy after different treatments. It can be seen from the figure that the hardness of as-cast magnesium alloy is low, and the change of hardness after T6 heat treatment is not obvious. However, after extrusion, the hardness of the alloy has been greatly improved. Compared with the casting, its hardness has increased by 24.3%. This is mainly because the extrusion causes the alloy to produce large plastic deformation, its internal structure is enhanced and the defects are effectively reduced.

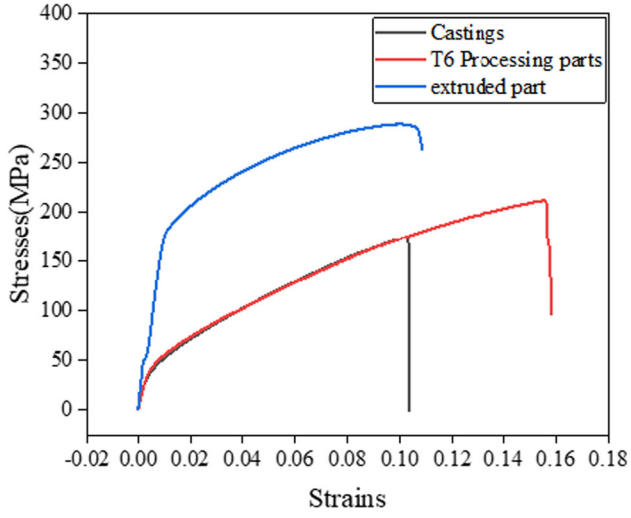

Fig. 5 The stress-strain curve of Mg-1Mn-2Zn alloy

Table 1 Summary of tensile strength and elongation of different strengthening alloys

Name	Tensile strength, MPa	Elongation, %
Mg-1Mn-2Zn-castings	174.20	10.88
Mg-1Mn-2Zn-T6	212.02	15.78
Mg-1Mn-2Zn-extruded	288.92	16.67

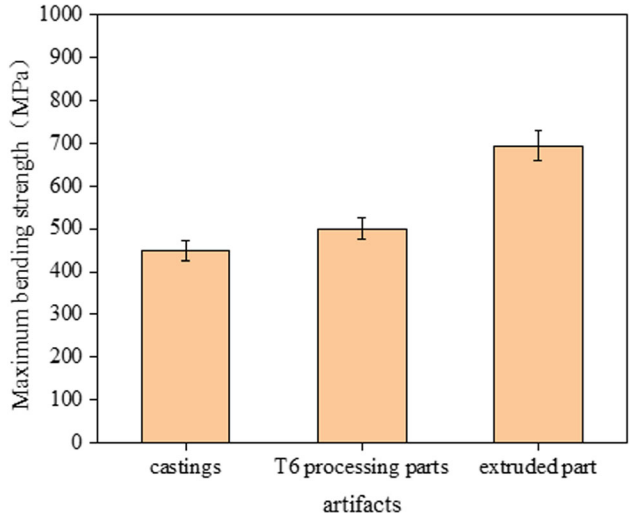

Fig. 6 Maximum bending strength of Mg-Mn-Zn alloy

3.2 Comparison of Residual Stress Test of Alloy

The residual stress of magnesium alloy in different treatment states was tested. It can be seen from Fig. 4 that the residual stress value of magnesium alloy changed after heat treatment, but it was not obvious. The residual stress of castings and heat treatment parts fluctuated around 0. The alloy produced a large residual compressive stress after extrusion, which helped to refine the grains of the alloy and improve the hardness and strength of the alloy surface.

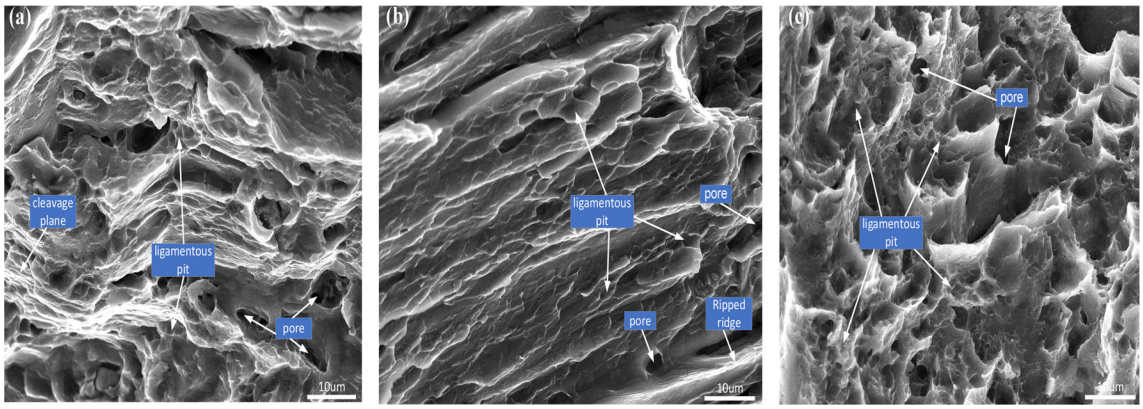

Fig. 7 Analysis of tensile fracture morphology (a) casting (b) T6 treatment part (c) extrusion part

3.3 Tensile and Bending Test Analysis

3.3.1 Tensile Test Analysis. The stress-strain curves of Mg-1Mn-2Zn alloy with different treatment methods are shown in Fig. 5. It can be seen from the figure that T6 heat treatment has limited improvement on the properties of the alloy. It is only improved on the basis of the properties of the cast alloy itself, and the tensile strength and elongation of the magnesium alloy are improved. This is because the heat treatment is mainly to improve the internal defects of the cast alloy. On the basis of heat treatment, the alloy is further extruded and strengthened, which further strengthens the tensile strength of the alloy on the basis of heat treatment. The maximum tensile strength can reach 288.92 MPa, which is about 65.9% higher than that of the cast alloy, which greatly improves the mechanical properties of the magnesium alloy. The tensile strength and elongation of different strengthening alloys are shown in Table 1.

3.3.2 Bending Test Analysis. As shown in Fig. 6, the maximum bending strength of magnesium alloy has been improved after heat treatment and extrusion strengthening, which indicates that the composite strengthening can better improve the mechanical properties of the alloy. After extrusion, the bending strength of magnesium alloy increases more. This may be because extrusion can refine the grains of magnesium alloy and enhance the internal structure. The bending test further proves that the overall mechanical properties of magnesium alloy are improved, which is basically consistent with the experimental results of tension.

3.3.3 Fracture Morphology Analysis. The fracture morphology of tensile and bending fracture is shown in Fig. 7 and 8. From the figure, we can see that in the casting stage, there are a large number of cleavage planes and tearing ridges in the material, which are some characteristics of brittleness of the material, but there are also a few dimples. Even in the fracture of bending fracture, some fish-scale dimple groups can be seen, but these dimples are relatively shallow and not obvious. This is mainly because there is a small amount of Mn element in the alloy. The existence of Mn element can improve the tensile properties of magnesium alloy to a certain extent, so that the alloy has certain plastic characteristics. After heat treatment, the pore defects of the material itself have been effectively reduced, and the number of dimples has also been increased correspondingly, but there are still some brittle fracture characteristics such as intergranular fracture and tearing ridge. After extrusion strengthening, the number of dimples at the fracture has been greatly increased. The fracture characteristics of the alloy at this time are mainly plastic fracture. The SEM images of tensile fracture morphology and bending fracture morphology show such changes, which is also consistent with the results of tensile and bending tests.

3.3.4 Physical Phase Analysis. The XRD scanning pattern of magnesium alloy is shown in Fig. 9, from the XRD diffraction pattern, it can be seen that the physical phase is dominated by α-Mg, and the peaks appeared in the intermetallic phases such as MgZn, $MgZn_2$ and Mg_2Zn_3, which indicates that the eutectic transformation of magnesium alloy has occurred in the process of casting, heat treatment and extrusion, and the formation of the intermetallic phases of MgZn, $MgZn_2$ and Mg_2Zn_3 intermetallic phases is conducive to the enhancement of the mechanical properties and corrosion resistance of the magnesium alloy. However, the phase containing Mn element was not formed, which is mainly because the content of added Mn element is small, and the influence on the generation of phase organization is small so that there is no phase generation of Mn.

3.4 Wear Resistance Analysis

Fretting is a kind of movement with very small relative displacement. After the bone plate is implanted into the human body, there will be more or less fretting between the bone plate and the human bone due to the activities of the human body. Therefore, it is necessary to study the fretting wear performance of magnesium alloy. The change of fretting wear friction coefficient of Mg-Mn-Zn alloy in different treatment states is shown in Fig. 10. It can be seen from the change of the friction coefficient curve that the fretting wear is mainly divided into three stages, namely the rapid rise stage-slow rise stage-stable wear stage. This is mainly because in the early stage of wear, with the increase of the loading force, the surface of the alloy will produce wear debris and the wear state is complex and changeable. With the progress of friction, the surface will gradually stabilize and gradually enter the stage of stable wear. It can be seen from Fig. 10 and Table 2 that after T6 aging treatment, the friction coefficient of the alloy is improved. This is because after heat treatment, although the hardness of the alloy is improved, its performance improvement is limited. At the same time, the casting and heat treatment parts still have defects, resulting in the occurrence of adhesive wear in both states of the alloy, resulting in a higher friction coefficient of the workpiece of the heat-treated magnesium alloy. After extrusion

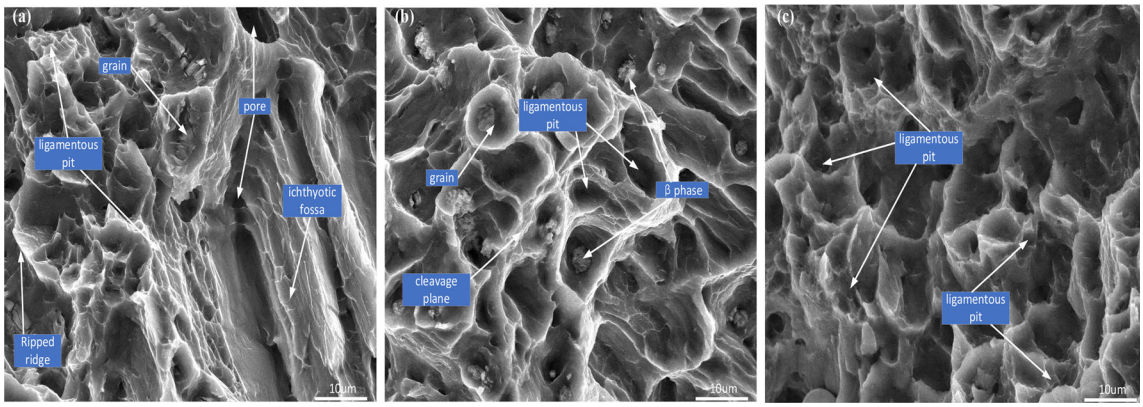

Fig. 8 Bending fracture morphology analysis (a) casting (b) T6 treatment (c) extrusion

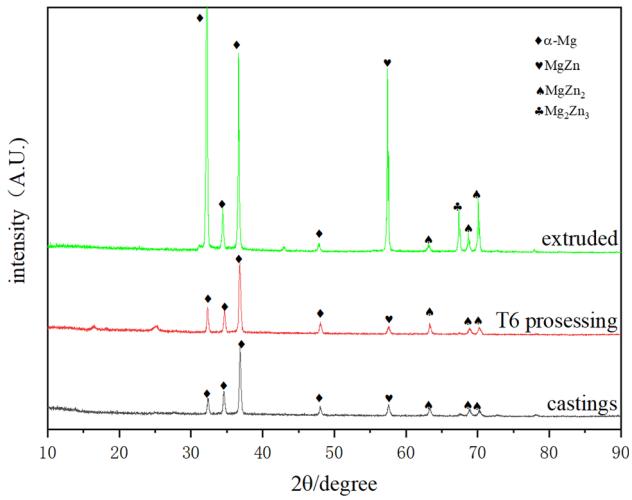

Fig. 9 Physical phase analysis of magnesium-manganese-zinc alloys

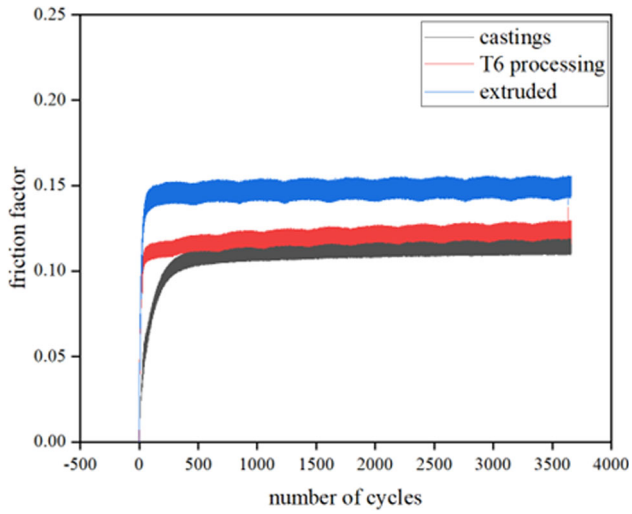

Fig. 10 Comparison of fretting wear friction coefficient of magnesium alloy

strengthening, the overall performance of the alloy is greatly improved, which makes up for the deficiency of heat treatment, The coefficient of friction of the alloy is not significantly reduced, but this does not mean that the wear resistance of the alloy is not significantly reduced. To further understand the change in the wear resistance of the alloy, it is necessary to further look at the change in the size of the alloy wear pits.

Table 2 Friction factor and maximum pit depth of different strengthened alloys

Name	Friction factor	Maximum pit depth
Mg-1Mn-2Zn-castings	0.0905	− 20.0
Mg-1Mn-2Zn-T6	0.1393	− 33.8
Mg-1Mn-2Zn-extruded	0.1472	− 9.8

Figure 11 shows the fretting wear Ft-D-N curve. It can be seen from the figure that although the alloy has been treated in different ways, the shape of their curves is elliptical, but the elliptical shape is more obvious after extrusion. This indicates that the fretting of Mg-Mn-Zn alloy is carried out in the mixed zone, that is, the fretting is in the state of coexistence of complete slip and partial slip. It can be seen from the change of the curve that after a certain period of reciprocating fretting, the curve gradually reaches a steady state, and no obvious change occurs. At this time, the fretting wear is in the elastic adjustment mixed zone.

Figure 12 shows the fretting wear pit morphology and surface scanning contour map of magnesium alloy in three states. It can be seen from the figure that the overall depth and area of the wear pit of the extruded magnesium manganese zinc alloy are significantly reduced, mainly because the mechanical properties such as strength and hardness of the alloy are significantly improved after extrusion. It can be seen from the depth profile of the wear pit of the magnesium alloy that a deeper tear pit appears in the wear pit of the magnesium alloy after T6 aging treatment, which indicates that the adhesion phenomenon occurs between the magnesium alloy substrate and the friction pair during the wear process. The friction pair brings up the material on the magnesium alloy substrate during movement, and tear occurs, which also confirms that the alloy has adhesive wear after heat treatment. It can also be seen that there is also a small degree of adhesive wear during the fretting process of the casting. This is mainly because the hardness and strength of the casting itself are not high, and there are many defects. Therefore, there are fewer matrix materials torn during the wear process, and the degree of adhesive wear is lighter.

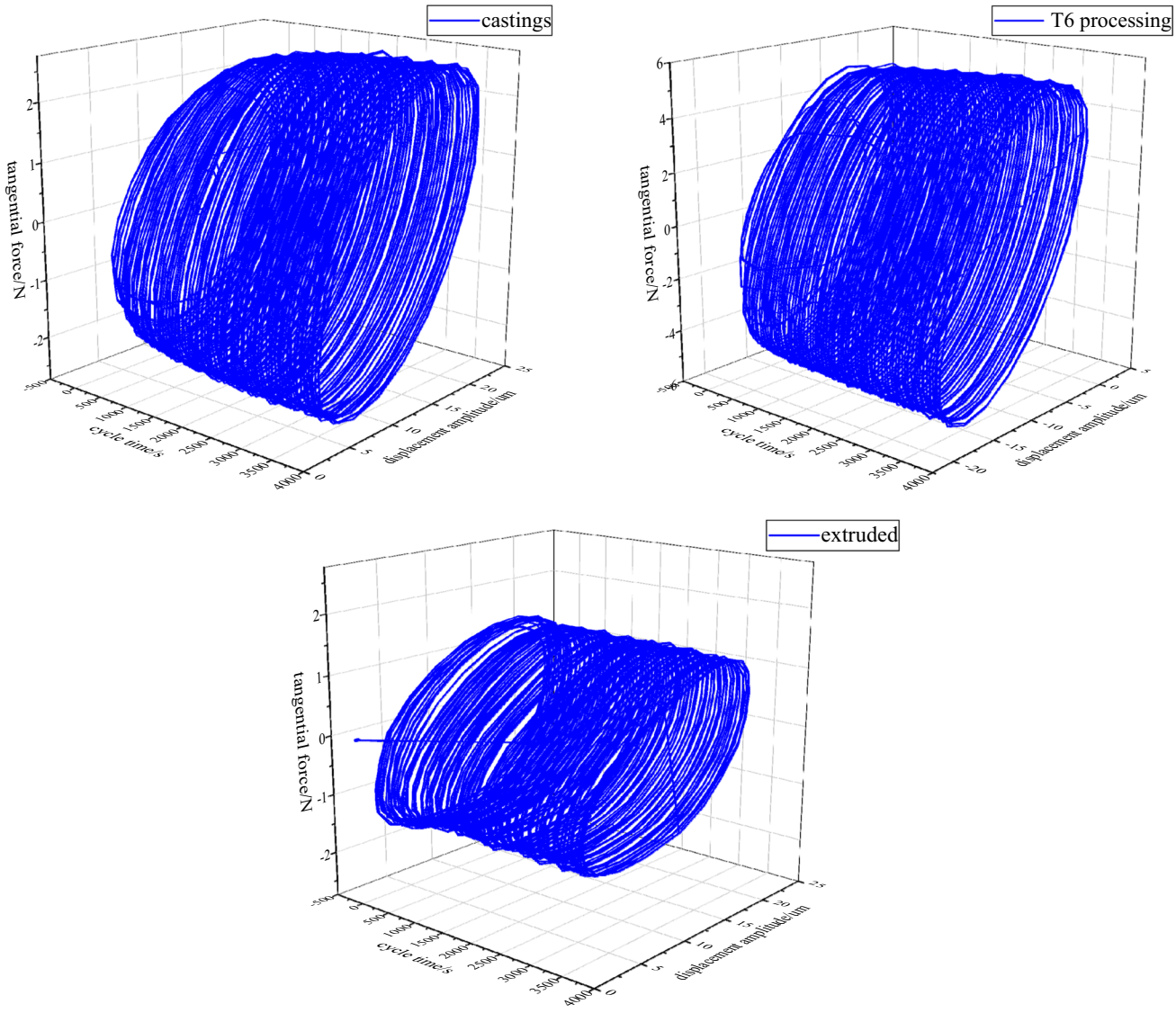

Fig. 11 Comparison of fretting friction rings of three different states of magnesium alloy

3.5 Analysis of Corrosion Resistance

The corrosion resistance of magnesium alloy has always been a very important aspect of its application in medical research. After strengthening the magnesium alloy in different ways, the corresponding corrosion resistance will also change. The Tafel polarization curve of the electrochemical corrosion test of Mg-1Mn-2Zn alloy is shown in Fig. 13, and the parameters of the polarization curve are shown in Table 3. The results show that the heat treatment of the casting can't effectively improve the corrosion resistance of the alloy, but the extrusion strengthening of the alloy after heat treatment can effectively improve the corrosion potential of the magnesium manganese zinc alloy and reduce the corrosion current density, which shows that the extrusion strengthening can effectively improve the corrosion resistance of the alloy. Detailed information on electrochemical corrosion rate calculations can be obtained from the ASTM G102-89 standard. The calculation formula is as in (4) (Ref 29):

$$C_R = \frac{k_1 j_{\text{corr}} E_w}{\rho} \quad \text{(Eq 4)}$$

where: k_1 is the fixation factor with a value of 3.27×10^{-3} (mm g/μA·cm yr.); j_{corr} is the corrosion current density; ρ is the density, which is 1.8 g/cm^3 for magnesium alloys; and the E_w value is 21.629. The change in corrosion rate in Table 3 shows that heat treatment did not enhance the corrosion resistance of Mg-Mn-Zn alloy, while extrusion strengthening can effectively enhance the corrosion resistance of the alloy.

3.6 Analysis of Corrosion Products

Because this paper only carried out different strengthening treatments on Mg-Mn-Zn alloy, there was no addition and change of any other elements and composition content in the strengthening process, and the corrosion products of the alloy were the same. Therefore, only the corrosion products of the alloy after T6 and extrusion composite strengthening treatment were analyzed by XPS. Figure 14 shows the fitting results of the corrosion products of Mg-Mn-Zn alloy. Through the full energy spectrum, it can be seen that the corrosion products mainly contain C, O, Mg, Mn, Zn, Cl and P elements.

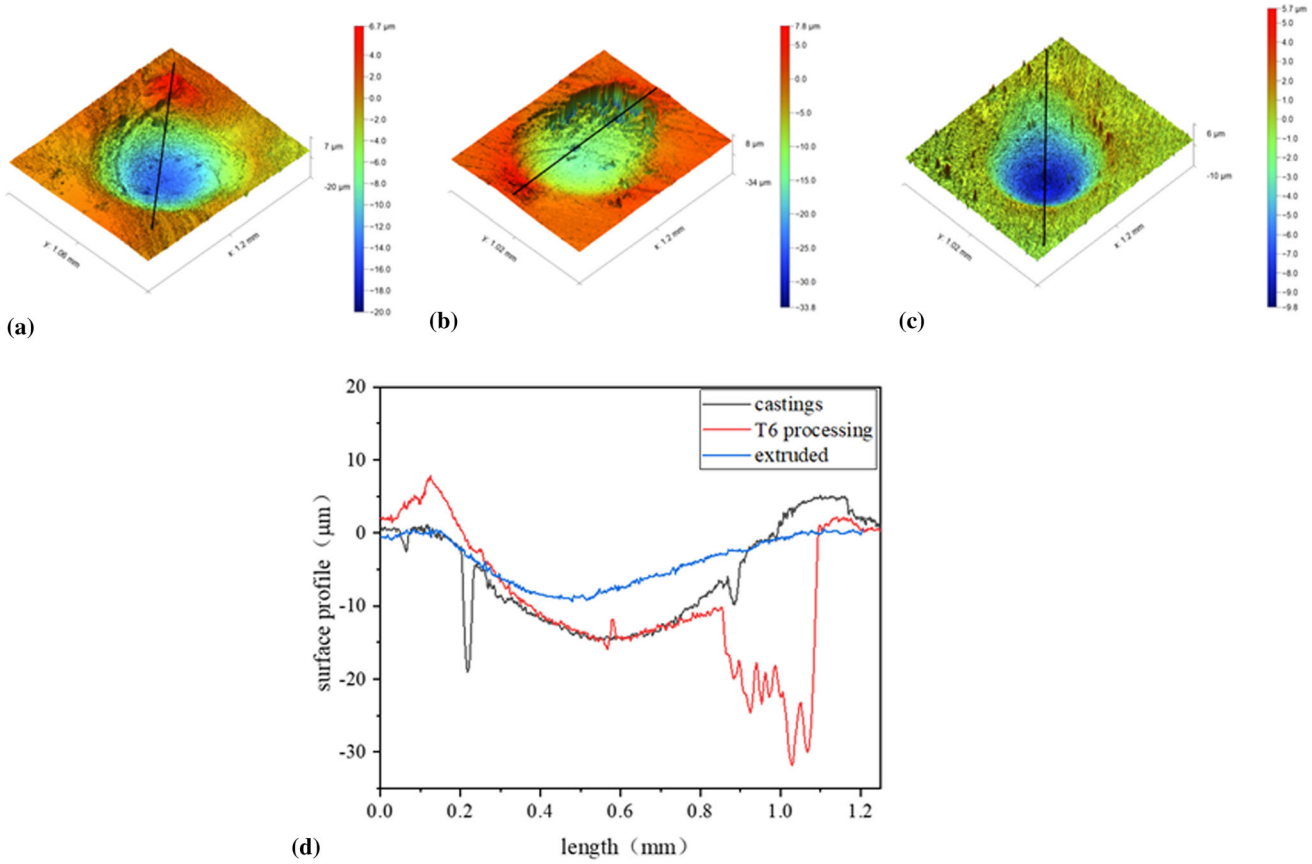

Fig. 12 Wear scar morphology and surface scanning contour map of magnesium alloy (a) casting (b) T6 treated part (c) extrusion part (d) scanning contour map

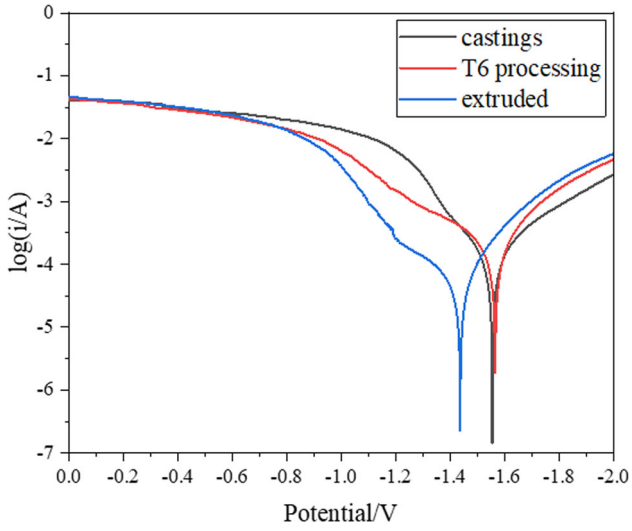

Fig. 13 Electrochemical corrosion polarization curve of Mg-Mn-Zn alloy

Through Fig. 14(b), it can be seen that C1s shows two peaks. According to the binding energy of the peaks, it can be seen that C exists in the form of CO_3^{2-} according to the electron energy spectrum manual. Figure 14(c) shows the fine spectrum of O 1*s*. It can be seen that the O element is mainly in the form of carbonate and hydroxide, so its ion is in the form of O^{2-}. The fine spectrum of Mg 2*p* is shown in Fig. 14(d). Since

Table 3 Polarization curve parameters of Mg-1Mn-2Zn alloy (φ_{corr} corrosion potential, J_{corr} corrosion current density)

Name	φ_{corr}, V	J_{corr}, A cm^2	Corrosion rate C_R, mm/yr.
Mg-1Mn-2Zn-castings	− 1.554	1.259×10^{-4}	4.947
Mg-1Mn-2Zn-T6	− 1.564	1.664×10^{-4}	6.538
Mg-1Mn-2Zn-extruded	− 1.436	5.394×10^{-5}	2.119

the chemical properties of Mg are very active, there is no elemental magnesium on the surface of the alloy after corrosion, and the corrosion products are mainly $MgCO_3$, $Mg(OH)_2$ and MgO. The electron energy spectra of Mn 2*p* and Zn 2*p* are shown in (e) and (f). It can be seen that Mn 2*p* and Zn 2*p* have obvious spin orbit components (Δ_{Mn} = 11.2 eV, Δ_{Zn} = 23 eV), that is, there are two peaks. Combined with other electron energy spectra and electron energy spectrum manuals, it can be seen that the corrosion products may include MnO, ZnO, $MnCl_2$, Zn $(OH)_2$ and other compounds, so Mn and Zn elements exist in the form of divalent ion state. The electronic energy spectrum of Cl 2*p* is shown in Fig. 14(g). Combined with the binding energy of Cl^-, it can be seen that Cl element exists in the form of chloride, which is consistent with other electronic energy spectrum analysis. Figure 14(h) shows the

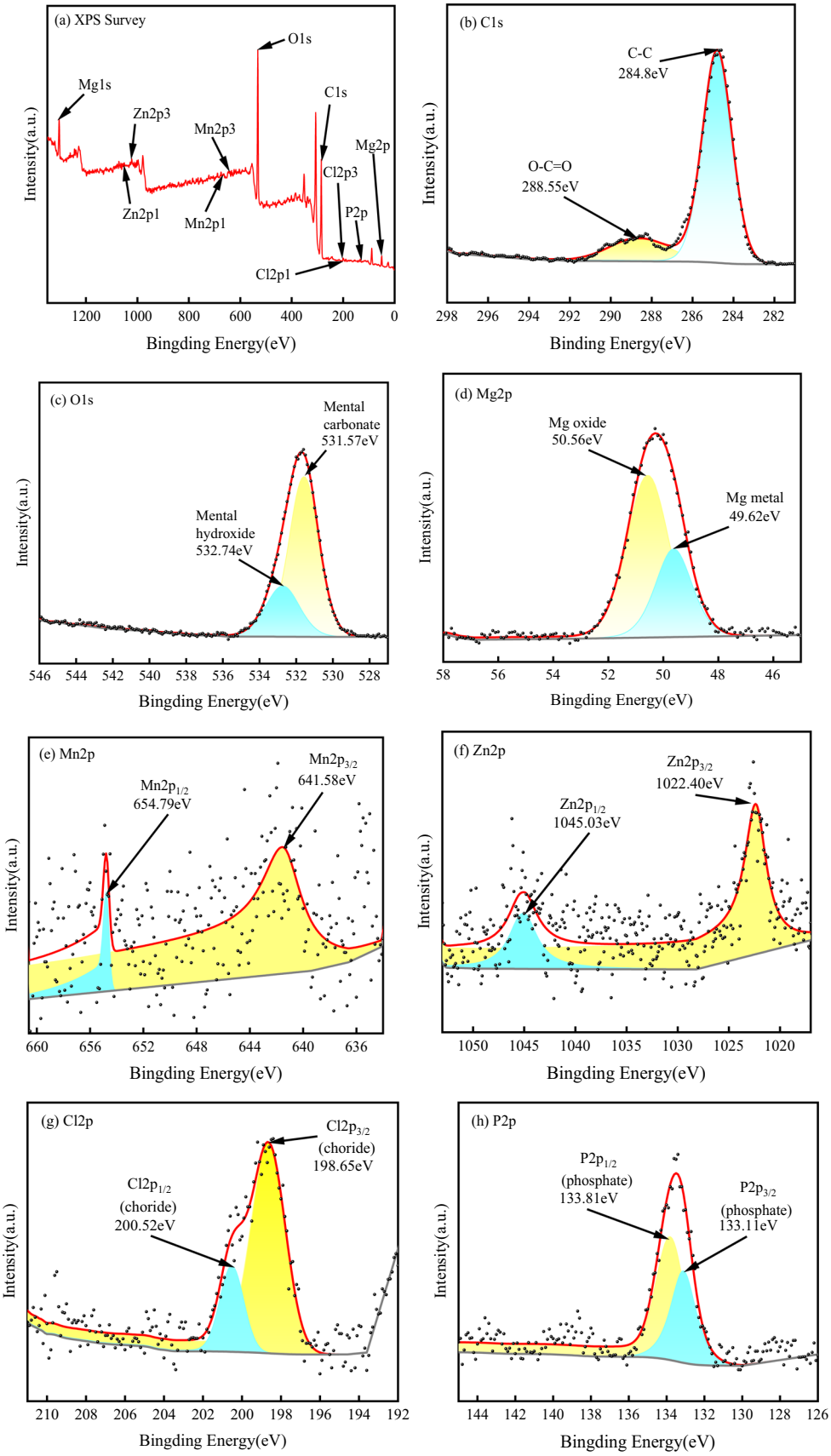

Fig. 14 XPS peak fitting of Mg-1Mn-2Zn alloy

Table 4 Types and binding energies of different elements of Mg-1Mn-2Zn

Peak value	Tyoe	Binding energy, eV
C 1*s*	C–C	284.8
	O–C=O	288.5
O 1*s*	CO_3^{2-}	531.5-532
	O^{2-}	529-530
Mg 2*p*	$Mg(OH)_2$	49.5
Mn 2*p*	MgO	50.8
	MnO	641.4
	$MnCl_2$	642.0
Zn 2*p*	Zn^{2+}	1021-1023
Cl 2*p*	Cl^-	198.5-199
P 2*p*	PO_4^{3-}	133

electron energy spectrum of P 2*p*. The binding energies of Na_2HPO_4 and NaH_2PO_4 are 133.1 and 134.2 eV, which indicates that PO43-exists in the corrosion products of magnesium alloy. The types and binding energies of different elements on the surface of magnesium alloy after corrosion are shown in Table 4. It can be seen from the above that the corrosion products of Mg-1Mn-2Zn alloy after corrosion are harmless to the human body and can be absorbed or discharged by the human body.

4. Conclusion

In this paper, the self-made Mg-1Mn-2Zn alloy was subjected to heat treatment and extrusion strengthening treatment. The effects of composite strengthening on the mechanical properties of the material were studied by hardness, residual stress test, tensile and bending tests. The effects of composite strengthening on the wear resistance and corrosion resistance of the material were studied by fretting wear test analysis and electrochemical corrosion test and corrosion product test analysis. The conclusions are as follows.

(1) Compared with the casting Mg-1Mn-2Zn, the hardness and residual compressive stress of the alloy were greatly improved after T6 treatment and extrusion strengthening. The maximum tensile strength reached 288.92 MPa, which was about 65.9% higher than that of the casting alloy, and the elongation was also greatly improved. It meets the needs of medical implantation of magnesium alloys with strength above 200 MPa and elongation above 10%.
(2) The fretting wear experiment of Mg-1Mn-2Zn alloy found that the abrasion resistance of the alloy gets better after the extrusion strengthening treatment, and the friction ring of the alloy showed more obvious elliptical characteristics. The area and depth of the wear pit were also effectively reduced, and the wear resistance was greatly improved.
(3) Electrochemical corrosion test confirmed that the composite strengthening is helpful to improve the corrosion resistance of magnesium alloy. The increase of corrosion potential and the decrease of current density prove that the corrosion resistance of magnesium alloy has been improved. And the annual corrosion rate of magnesium alloys was reduced after heat treatment and extrusion strengthening. XPS analysis confirms that the corrosion products of magnesium alloy after corrosion in simulated body fluid can be absorbed or excluded by human body, and will not have adverse effects on human body, with excellent degradability and biocompatibility.

Compared with other medical implantable magnesium alloys, the strength and ductility of Mg-1Mn-2Zn alloy are enhanced after strengthening, which meets the mechanical property requirements of medical implantable alloys, and the degradation products can be absorbed or degraded by the human body, so it has a greater application value.

Acknowledgments

This research was supported by the National Natural Science Foundation of China (52175408) and Shandong Provincial Natural Science Foundation (ZR2023ME077, ZR2023MC140).

References

1. M. Kalaiyarasan, S. Pugalmani, and N. Rajendran, Fabrication of Chitosan/Silica Hybrid Coating on AZ31 Mg Alloy for Orthopaedic Applications, *J. Magnes. Alloy*, 2023, **11**(2), p 614–628. https://doi.org/10.1016/j.jma.2022.05.003
2. I. Antoniac, M. Miculescu, V. Mănescu, A. Stere, P.H. Quan, G. Păltânea, A. Robu, and K. Earar, Magnesium-Based Alloys used in Orthopedic Surgery, *Materials*, 2022, **15**(3), p 1148. https://doi.org/10.3390/ma15031148
3. S. Pang, W. Zhao, T. Qiu, W. Liu, L. Jiao, and X. Wang, Study on Surface Quality and Mechanical Properties of Micro-Milling WE43 Magnesium Alloy Cardiovascular Stent, *J. Manuf. Process.*, 2023, **101**, p 1080–1090. https://doi.org/10.1016/j.jmapro.2023.06.061
4. P. Tong, Y. Sheng, R. Hou, M. Iqbal, L. Chen, and J. Li, Recent Progress on Coatings of Biomedical Magnesium Alloy, *Smart Mater. Med.*, 2022, **3**, p 104–116. https://doi.org/10.1016/j.smaim.2021.12.007
5. R. Hedayati, S.M. Ahmadi, K. Lietaert, N. Tümer, Y. Li, S. Amin Yavari, and A.A. Zadpoor, Fatigue and Quasi-Static Mechanical Behavior of Bio-Degradable Porous Biomaterials Based on Magnesium Alloys, *J. Biomed. Mater. Res. A*, 2018, **106**(7), p 1798–1811. https://doi.org/10.1002/jbm.a.36380
6. H. Zhou, B. Liang, H. Jiang, Z. Deng, and K. Yu, Magnesium-Based Biomaterials as Emerging Agents for Bone Repair and Regeneration: From Mechanism to Application, *J. Magnes. Alloy.*, 2021, **9**(3), p 779–804. https://doi.org/10.1016/j.jma.2021.03.004
7. Y. Zhang, J. Xu, Y.C. Ruan, M.K. Yu, M. O'Laughlin, H. Wise, D. Chen, L. Tian, D. Shi, J. Wang, S. Chen, J.Q. Feng, D.H.K. Chow, X. Xie, L. Zheng, L. Huang, S. Huang, K. Leung, N. Lu, L. Zhao, H. Li, D. Zhao, X. Guo, K. Chan, F. Witte, H.C. Chan, Y. Zheng and L. Qin, Implant-Derived Magnesium Induces Local Neuronal Production of CGRP to Improve Bone-Fracture Healing in Rats, *Nat. Med.*, 2016, **22**(10), p 1160–1169. https://doi.org/10.1038/nm.4162
8. A. Drynda, T. Hassel, R. Hoehn, A. Perz, F. Bach, and M. Peuster, Development and Biocompatibility of a Novel Corrodible Fluoride-Coated Magnesium-Calcium Alloy with Improved Degradation Kinetics and Adequate Mechanical Properties for Cardiovascular Applications, *J. Biomed. Mater. Res. A Off. J. Soc. Biomater. Jpn. Soc. Biomater. Aust. Soc. Biomater. Korean Soc. Biomater.*, 2010, **93**(2), p 763–775. https://doi.org/10.1002/jbm.a.32582
9. Y. Song, K. Yuan, X. Li, and Y. Qiao, Microstructure and Properties of Biomedical Mg-Zn-Ca Alloy at Different Extrusion Temperatures, *Mater. Today Commun.*, 2023, **35**, p 105578. https://doi.org/10.1016/j.mtcomm.2023.105578
10. D. Ding, J. Roth, and R. Salvi, Manganese is Toxic to Spiral Ganglion Neurons and Hair Cells In Vitro, *Neurotoxicology*, 2011, **32**(2), p 233–241. https://doi.org/10.1016/j.neuro.2010.12.003

11. B. Nami, S.M. Miresmaeili, F. Jamshidi, and I. Khoubrou, Effect of Ca Addition on Microstructure and Impression Creep Behavior of Cast AZ61 Magnesium Alloy, *Trans. Nonferrous Met. Soc. China*, 2019, **29**(10), p 2056–2065. https://doi.org/10.1016/S1003-6326(19)65112-5
12. D. Yin, E. Zhang, and S. Zeng, Effect of Zn on Mechanical Property and Corrosion Property of Extruded Mg-Zn-Mn Alloy, *Trans. Nonferrous Met. Soc. China*, 2008, **18**(4), p 763–768. https://doi.org/10.1016/S1003-6326(08)60131-4
13. M. Němec, A. Jäger, K. Tesař, and V. Gärtnerová, Influence of Alloying Element Zn on the Microstructural, Mechanical and Corrosion Properties of Binary Mg-Zn Alloys After Severe Plastic Deformation, *Mater Charact*, 2017, **134**, p 69–75. https://doi.org/10.1016/j.matchar.2017.10.017
14. P. Metalnikov, G. Ben-Hamu, Y. Templeman, K.S. Shin, and L. Meshi, The Relation Between Mn Additions, Microstructure and Corrosion Behavior of New Wrought Mg-5Al Alloys, *Mater Charact*, 2018, **145**, p 101–115. https://doi.org/10.1016/j.matchar.2018.08.033
15. F. Rosalbino, S.D. Negri, G. Scavino, and A. Saccone, Microstructure and In Vitro Degradation Performance of Mg–Zn–Mn Alloys for Biomedical Application, *J. Biomed. Mater. Res. A*, 2013, **101**(3), p 704–711. https://doi.org/10.1002/jbm.a.34368
16. M. Erinc, W.H. Sillekens, R.G.T.M. Mannens, R.J. Werkhoven, Applicability of Existing Magnesium Alloys as Biomedical Implant Materials, in TMS Annual Meeting & Exhibition, 2009
17. Y. Sun, B. Zhang, Y. Wang, L. Geng, and X. Jiao, Preparation and Characterization of a New Biomedical Mg–Zn–Ca Alloy, *Mater. Des.*, 2012, **34**, p 58–64. https://doi.org/10.1016/j.matdes.2011.07.058
18. H. Li, D. Liu, Y. Zhao, F. Jin, and M. Chen, The Influence of Zn Content on the Corrosion and Wear Performance of Mg-Zn-Ca Alloy in Simulated Body Fluid, *J. Mater. Eng. Perform.*, 2016, **25**, p 3890–3895. https://doi.org/10.1007/s11665-016-2207-0
19. X. Gong, J. Chen, H. Yan, W. Xia, and B. Su, Effects of Aging Treatment and Pre-Deformation on Stress Corrosion Cracking of Magnesium Alloy, *J. Mater. Res. Technol.*, 2023, **22**, p 2844–2861. https://doi.org/10.1016/j.jmrt.2022.12.129
20. J. Zheng, Z. Yan, Q. Wang, Z. Zhang, and Y. Xue, Microstructure and Texture Evolution of AZ31 Alloy Prepared by Cyclic Expansion Extrusion with Asymmetrical Extrusion Cavity at Different Temperatures, *Materials*, 2020, **13**(17), p 3757. https://doi.org/10.3390/ma13173757
21. T. Nakata, C. Xu, K. Kaibe, Y. Yoshida, K. Yoshida, and S. Kamado, Improvement of Strength and Ductility Synergy in a Room-Temperature Stretch-Formable Mg-Al-Mn Alloy Sheet by Twin-Roll Casting and Low-Temperature Annealing, *J. Magnes. Alloy*, 2022, **10**(4), p 1066–1074. https://doi.org/10.1016/j.jma.2021.07.017
22. X. Lin, Z. Chen, J. Shao, J. Xiong, Z. Hu, and C. Liu, Deformation Mechanism, Orientation Evolution and Mechanical Properties of Annealed Cross-Rolled Mg-Zn-Zr-Y-Gd Sheet During Tension, *J. Magnes. Alloy*, 2021 https://doi.org/10.1016/j.jma.2021.08.006
23. B.N. Du, Z.Y. Hu, L.Y. Sheng, D.K. Xu, Y.X. Qiao, B.J. Wang, J. Wang, Y.F. Zheng, and T.F. Xi, Microstructural Characteristics and Mechanical Properties of the Hot Extruded Mg-Zn-Y-Nd Alloys, *J. Mater. Sci. Technol.*, 2021, **60**, p 44. https://doi.org/10.1016/j.jmst.2020.05.021
24. T.O. Sadiq, I. Sudin, A. Alsakkaf, J. Idris, and N.A. Fadil, Effect of Homogenization Heat Treatment on the Microstructure of AZ91 Magnesium Alloy at Different Temperatures and Ageing Times, *J. Eng. Res.*, 2023 https://doi.org/10.1016/j.jer.2023.100133
25. L.Y. Sheng, B.N. Du, Z.Y. Hu, Y.X. Qiao, Z.P. Xiao, B.J. Wang, D.K. Xu, Y.F. Zheng, and T.F. Xi, Effects of Annealing Treatment on Microstructure and Tensile Behavior of the Mg-Zn-Y-Nd Alloy, *J. Magnes. Alloy*, 2020, **8**(3), p 601–613. https://doi.org/10.1016/j.jma.2019.07.011
26. F. Kiani, J. Lin, A. Vahid, K. Munir, C. Wen, and Y. Li, Microstructures, Mechanical Properties, Corrosion, and Biocompatibility of Extruded Mg-Zr-Sr-Ho Alloys for Biodegradable Implant Applications, *J. Magnes. Alloy*, 2023, **11**(1), p 110–136. https://doi.org/10.1016/j.jma.2022.10.002
27. B. Du, Z. Hu, J. Wang, L. Sheng, H. Zhao, Y. Zheng, and T. Xi, Effect of Extrusion Process on the Mechanical and In Vitro Degradation Performance of a Biomedical Mg-Zn-Y-Nd Alloy, *Bioact. Mater.*, 2020, **5**(2), p 219–227. https://doi.org/10.1016/j.bioactmat.2020.02.002
28. S. Zhang, X. Zhang, C. Zhao, J. Li, Y. Song, C. Xie, H. Tao, Y. Zhang, Y. He, Y. Jiang, and Y. Bian, Research on an Mg–Zn Alloy as a Degradable Biomaterial, *Acta Biomater.*, 2010, **6**(2), p 626–640. https://doi.org/10.1016/j.actbio.2009.06.028
29. ASTM International, in Annual Book of ASTM Standards, 2010, **89**, p 1–7